

# Changes in the Contact Stress Distribution Pattern of the Patellofemoral Joint After Medial Open-Wedge High Tibial Osteotomy

## An Evaluation Using Computed Tomography Osteoabsorptiometry

Toshiaki Kameda,\* MD, Eiji Kondo,<sup>†‡</sup> MD, PhD, Tomohiro Onodera,\* MD, PhD, Koji Iwasaki,<sup>§</sup> MD, PhD, Jun Onodera,<sup>||</sup> MD, PhD, Kazunori Yasuda,<sup>||</sup> MD, PhD, and Norimasa Iwasaki,\* MD, PhD

*Investigation performed at the Centre for Sports Medicine, Hokkaido University Hospital, Sapporo, Hokkaido, Japan*

**Background:** Medial open-wedge high tibial osteotomy (OWHTO) theoretically causes distalization and lateralization of the tibial tuberosity and the patella.

**Purpose/Hypothesis:** The purpose of the study was to identify any changes in the stress distribution of subchondral bone density across the patellofemoral (PF) joint before and after OWHTO through the use of computed tomography (CT) osteoabsorptiometry. We hypothesized that OWHTO would alter the distribution of contact stress in the PF joint.

**Study Design:** Case series; Level of evidence, 4.

**Methods:** A total of 17 patients (17 knees) who underwent OWHTO were enrolled in this study between September 2013 and September 2015. All patients underwent radiologic examination preoperatively and at 1 year postoperatively, and the distribution patterns of subchondral bone density through the articular surface of the femoral trochlea and patella were assessed preoperatively and >1 year postoperatively using CT osteoabsorptiometry. The quantitative analysis of the obtained mapping data focused on location of the high-density area (HDA) through the articular surface of the PF joint. The percentage of HDA at each divided region of the articular surface of the femoral trochlea and the patella was calculated.

**Results:** In the radiologic evaluation, the Blackburne-Peel ratio was significantly reduced ( $P < .001$ ) after surgery, and the tilting angle of the patella was significantly decreased ( $P < .001$ ). On CT evaluation, the percentage of HDA in the lateral notch and lateral trochlea of the femur and in the medial portion of the lateral facet of the patella increased significantly after OWHTO surgery ( $P \leq .038$ ).

**Conclusion:** OWHTO significantly increased the stress distribution pattern of the lateral trochlea of the femur and the medial portion of the lateral facet of the patella. The procedure significantly lowered the patellar height and significantly decreased the patellar tilting angle after surgery.

**Keywords:** high tibial osteotomy; knee osteoarthritis; patellofemoral joint; medial open-wedge

Medial open-wedge high tibial osteotomy (OWHTO) has attracted a great deal of attention,<sup>17,34</sup> and favorable short-term results have been reported.<sup>1,25,28,30,31</sup> However, the patellar height has been found to decrease after

OWHTO surgery.<sup>3,10</sup> Reduction of the patellar height may lead to postoperative complications, such as anterior knee pain (AKP), patellar locking, crepitus, and limitation of knee motion.<sup>16,35</sup> Eventually, the altered patellofemoral (PF) congruency and contact stress may lead to PF joint osteoarthritis (OA).<sup>11</sup> Previous studies have revealed a decrease in lateral patellar tilt after OWHTO.<sup>8,16</sup> These results indicate that OWHTO may alter stress distribution

The Orthopaedic Journal of Sports Medicine, 9(4), 2325967121998050  
DOI: 10.1177/2325967121998050  
© The Author(s) 2021

This open-access article is published and distributed under the Creative Commons Attribution - NonCommercial - No Derivatives License (<https://creativecommons.org/licenses/by-nc-nd/4.0/>), which permits the noncommercial use, distribution, and reproduction of the article in any medium, provided the original author and source are credited. You may not alter, transform, or build upon this article without the permission of the Author(s). For article reuse guidelines, please visit SAGE's website at <http://www.sagepub.com/journals-permissions>.

across the PF joint. However, no in vivo studies have been conducted to clarify the stress distribution patterns of the PF joint after OWHTO.

To evaluate the effect of OWHTO on the actual loading condition of the PF joint, a reasonable analytical approach is needed to predict the characteristics of stress distribution based on in vivo imaging data obtained from living participants. Computed tomography (CT) osteoabsorptiometry was developed by Müller-Gerbl et al<sup>23,24</sup> to assess long-term stress distribution in individual joints of living participants by measuring subchondral bone density. Previous studies using this method have evaluated stress distribution at each joint under various loading conditions, from normal to pathologic conditions during athletic activity.<sup>5-7,13,26,27,29</sup> Hence, in this study we used CT osteoabsorptiometry to determine whether there were any changes in the stress distribution of subchondral bone density across the PF joint before and after OWHTO. We hypothesized that OWHTO would alter the distribution of contact stress in the PF joint.

## METHODS

### Study Design

This study involved patients who underwent OWHTO using locking plates (TomoFix [DePuy Synthes] or a TriS Medial HTO plate system [Olympus Terumo Biomaterials]) between September 2013 and September 2015. A single senior orthopaedic surgeon (E.K.), who was sufficiently trained concerning the procedure, performed all operations, inclusion criterion for the current study was symptomatic varus deformity of the knee after nonoperative treatment for 3 months or more. Exclusion criteria were (1) lateral femorotibial angle (FTA)  $>185^{\circ}$ <sup>28,33,39</sup> (neutral range,  $174^{\circ}$ - $178^{\circ}$ <sup>4,22,37</sup>); (2) extension loss  $>15^{\circ}$ ; (3) range of knee motion  $<130^{\circ}$ ; (4) history of infection in the knee before surgery; (5) preoperative OA in the PF joint classified as Kellgren-Lawrence<sup>15</sup> grade  $>3$ ; and (6) anterior cruciate ligament insufficiency or varus/valgus instability of  $>10^{\circ}$ . The references indicate the description of the FTA. There were no age restrictions.<sup>9</sup> The study protocol was approved by an institutional review board, and each participant provided informed consent.

A total of 18 patients (18 knees) were enrolled in this study. We evaluated the patients in our outpatient clinic for 1 year or more after surgery; 1 patient did not complete follow-up. Thus, a total of 17 patients (17 knees)

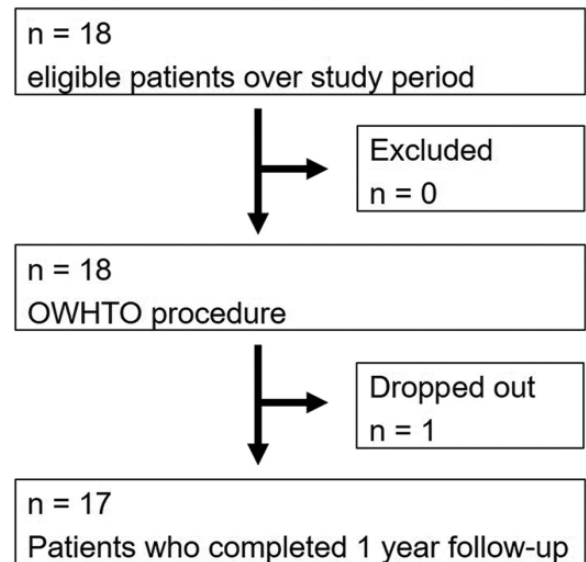


**Figure 1.** Flowchart for patients with inclusion and exclusion criteria. OWHTO, open-wedge high tibial osteotomy.

participated in this study and underwent CT and radiologic evaluations (Figure 1).

All patients underwent evaluation via the CT osteoabsorptiometry method based on the results of CT as the primary outcome. As a secondary outcome, patients underwent radiologic examinations before and 1 year after surgery.

### Surgical OWHTO Procedure

Diagnostic arthroscopy was performed using standard anterolateral and anteromedial parapatellar portals to confirm the presence of an isolated medial compartment OA. Concomitant procedures were performed to address medial compartment chondral injury or meniscal disease. We found 10 cases of meniscal injury requiring partial resection. Degenerative findings were observed in the medial menisci of all cases. Partial meniscectomy was performed for unstable meniscal tears in 10 knees. Debridement was performed for fragmentation of the cartilage. No treatment was administered for softening or fissuring of the articular cartilage.

This surgery was performed using the original procedure reported in 2014.<sup>28</sup> The proximal tibia was exposed via a

<sup>†</sup>Address correspondence to Eiji Kondo, MD, PhD, Centre for Sports Medicine, Hokkaido University Hospital, Kita-14, Nishi-5, Kita-ku, Sapporo 060-8648, Hokkaido, Japan (email: eijik@med.hokudai.ac.jp).

<sup>\*</sup>Department of Orthopaedic Surgery, Faculty of Medicine and Graduate School of Medicine, Hokkaido University, Sapporo, Hokkaido, Japan.

<sup>‡</sup>Centre for Sports Medicine, Hokkaido University Hospital, Sapporo, Hokkaido, Japan.

<sup>§</sup>Department of Functional Reconstruction for the Knee Joint, Faculty of Medicine, Hokkaido University, Sapporo, Hokkaido, Japan.

<sup>||</sup>Knee Research Center, Yagi Orthopaedic Hospital, Sapporo, Hokkaido, Japan.

Final revision submitted October 18, 2020; accepted November 30, 2020.

One or more of the authors has declared the following potential conflict of interest or source of funding: This work was supported in part by a grant-in-aid for scientific research (19K12746) from the Ministry of Education, Culture, Sports, Science and Technology of Japan. AOSSM checks author disclosures against the Open Payments Database (OPD). AOSSM has not conducted an independent investigation on the OPD and disclaims any liability or responsibility relating thereto.

Ethical approval for this study was obtained from Hokkaido University Hospital No. 017-0163.

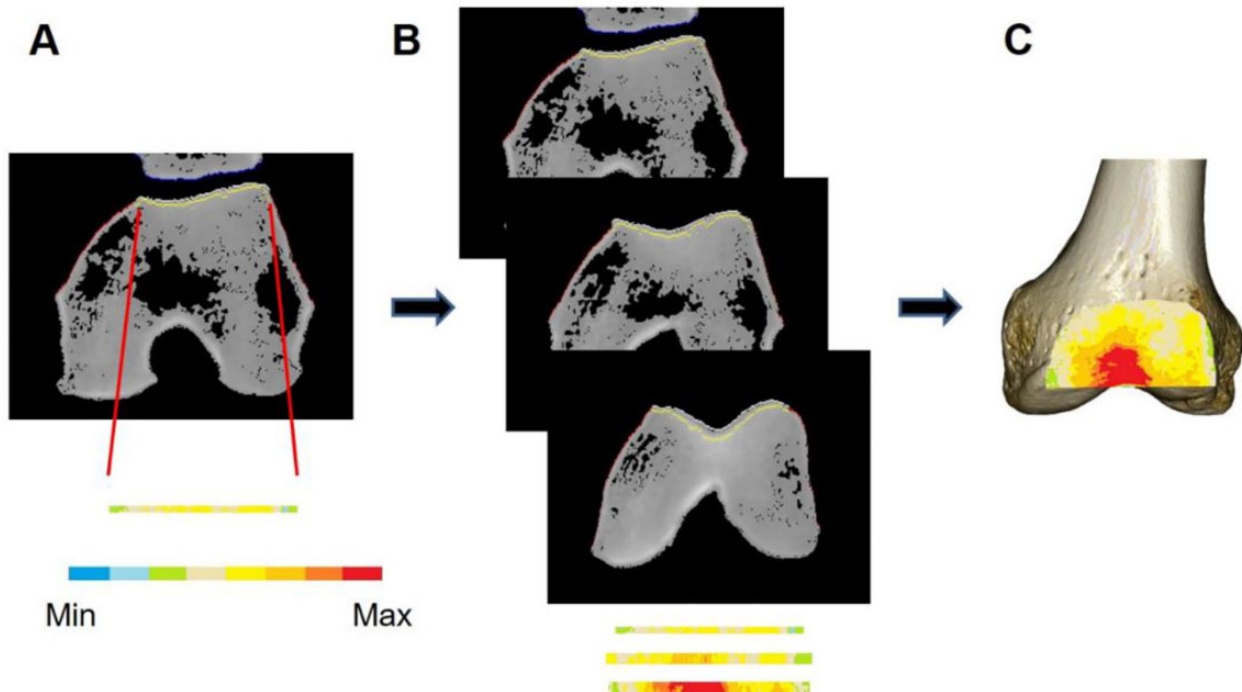


**Figure 2.** (A) The subchondral bone region of the patellofemoral articular surface of the distal femur is automatically identified using our original software. In each axial slice, the Hounsfield units of the identified region are measured at each coordinate point. (B) Distribution of the subchondral bone density is determined by stacking the data obtained from axial slices. (C) For quantitative analysis, the distribution pattern is represented as a surface mapping image depicted by 8-grade color scale. Min, minimum; Max, maximum.

7-cm medial longitudinal incision. Then, after complete release of the distal attachment of the superficial medial collateral ligament,<sup>33</sup> 3 pairs of Kirshner wires were inserted into the tibia so that each inserted Kirshner wire precisely reached the proximal tibiofibular joint using the parallel guide. Next, an ascending biplanar osteotomy of the tibial tubercle, which consisted of an oblique high tibial osteotomy (HTO) and a frontal plane osteotomy behind the tibial tubercle, was performed using an oscillating saw and chisel. The oblique osteotomy site was then gradually opened using a specially designed spreader (Olympus Terumo Biomaterials) under fluoroscopic control based on preoperative planning. Under fluoroscopic control, the surgeon confirmed that the mechanical axis of the corrected lower limb passed through the Fujisawa point (62.5%) on the tibial plateau using a long straight metal rod. Then, 2 wedge-shaped beta-tricalcium phosphate spacers (Osferion 60; Olympus Terumo Biomaterials) were implanted into the anterior and posterior parts of the opening space. Finally, the tibia was fixed using a locking plate (TomoFix or TriS Medial HTO plate system) by inserting 8 locking screws.

### Postoperative Rehabilitation

After surgery, all patients underwent postoperative management using the same rehabilitation protocol reported previously.<sup>28</sup> Straight leg raising and quadriceps setting

exercises as well as active and passive knee motion exercises were encouraged from the next day after surgery. Partial weightbearing on the tibia was permitted with crutches at 2 weeks after surgery. Full weightbearing was allowed at 4 weeks after surgery.

### CT Osteoabsorptiometry

CT (CT Highspeed Advantage; GE Healthcare) was performed before surgery and at 1 year after surgery. Slice thickness and intervals were set at 1 mm; the table speed was set at 1 mm/s. The CT scans of the knee were taken in a standard axial view. With the knee in full extension, scanning was performed from proximal to the patella to distal to the femur to access the PF joint. The acquired axial images were transferred to a personal computer, and a customized software program<sup>20</sup> was used for further analysis. The subchondral bone region of the PF articular surface of the distal femur was automatically identified using the software. Hounsfield units (HUs) of the identified subchondral bone region in each slice were measured at each coordinate point with 1-mm intervals (Figure 2A). Then, the distribution of subchondral bone density through the entire articular surface was created by stacking the measured data including the HU value at each coordinate point (Figure 2B). The range between the maximum and minimum HU values in each participant was divided into 8 equal grades, and a surface mapping

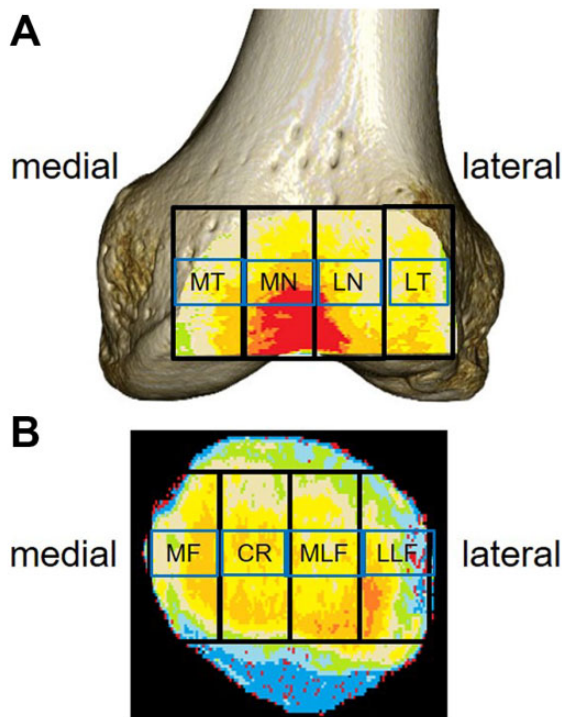


**Figure 3.** Divided regions of the (A) trochlea and (B) patella for quantitative analysis of the obtained mapping data. CR, central ridge; LLF, lateral portion of the lateral facet; LN, lateral notch; LT, lateral trochlea; MF, medial facet; MLF, medial portion of the lateral facet; MN, medial notch; MT, medial trochlea.

image depicted by the 8-grade color scale was created (Figure 2C).

The quantitative analysis of the obtained mapping data focused on location of the high-density area (HDA) through the articular surface. The HDA was defined as the area where the HU values are in the highest 2 grades. The percentage of HDA (%HDA) in each region was defined as the HDA of each divided region by the HDA of the entire articular surface. The %HDA at each divided region of the femoral trochlea and patellar articular surface was calculated. The divided regions of the trochlea included the lateral trochlea (LT), the lateral notch (LN), the medial notch (MN), and the medial trochlea (MT) (Figure 3A). The divided regions of the patella included the lateral portion of the lateral facet (LLF), the medial portion of the lateral facet (MLF), the central ridge, and the medial facet (MF) (Figure 3B).

### Radiologic Evaluation

The following radiologic outcomes were evaluated pre- and postoperatively. The FTA, defined as the angle between the anatomic axis of the femoral shaft and the axis of the tibial shaft on the fibular side, was measured on an anteroposterior (AP) weightbearing radiograph of a single leg with the knee joint in extension. The weightbearing line (WBL)

percentages and the entire leg length were measured on an AP radiograph of the entire lower limb taken using a long cassette in a single-leg standing position. To calculate the WBL, a line was drawn from the center of the femoral head to the middle point of the proximal talar joint surface. The WBL percentage was defined as the horizontal distance from the WBL to the medial edge of the tibial plateau, divided by the width of the tibial plateau. The Insall-Salvati ratio,<sup>12</sup> Blackburne-Peel ratio,<sup>2</sup> and posterior tibial slope<sup>21</sup> were estimated on lateral radiographs. The posterior tibial slope was measured as the angle between the line perpendicular to the mid-diaphysis of the tibia and the posterior inclination of the tibial plateau on the lateral view.

The patellar tilting angle,<sup>32</sup> lateral shift,<sup>32</sup> and congruence angle<sup>19</sup> were estimated on the skyline view with the knee flexed to 45°. The tilting angle was defined as the angle between the line intersecting the widest bony structure of the patella and the line tangentially passing the anterior surface of the femoral condyles. The lateral shift was defined as the ratio of the distance between the summit of the lateral femoral condyle and the point at which a line from the lateral edge of the patella, perpendicular to the line that passes through the summits of the femoral condyles, crosses that line to the distance between the summits of the medial and lateral femoral condyles of the femur. The congruence angle was defined as the angle between the line bisecting the sulcus angle and the line connecting the apex of the sulcus to the lowest part of the patellar ridge.

Osteoarthritic changes in the tibiofemoral (TF) joint were assessed on an AP radiograph of the knee according to the Kellgren-Lawrence<sup>15</sup> grading system. Osteoarthritic changes in the PF joint were assessed according to the Kellgren-Lawrence grading system on the skyline view with the knee flexed to 45°.

### Statistical Analysis

Sample size was based on a power analysis using data from our pilot and previous studies.<sup>26,29</sup> These studies showed a 10 percentage-point target difference in the mean value of percentage of low-density area (effect size) and an SD of <3 percentage points. A power analysis indicated that at least 5 participants were shown to have this effect size with 90% power and a significance of  $\alpha = .05$ . Therefore, 17 participants were enough for the current study. Statistical comparison of %HDA in each region and all radiographic findings between pre- and postoperative HTO groups was made using the paired Student *t* test. A commercially available software program (StatView; SAS Institute) was used for the statistical calculation. The significance level was set at  $P = .05$ .

To assess the consistency of the initial radiologic measurements, all parameters were remeasured at 48 to 72 hours after the initial evaluation. The test-retest reliability of the measurements was investigated by calculating the intraclass correlation coefficient (ICC; 2-way random model for agreement),<sup>18</sup> where an ICC of 0.75 to 1.00 shows excellent internal correlation.

TABLE 1  
Patient Characteristics (N = 17)

Variable	No. or Mean ± SD (Range)
Sex, male:female, n	5:12
Age, y	58.4 ± 9.4 (40-68)
Height, cm	161.7 ± 11.1 (150.0-183.0)
Body weight, kg	67.0 ± 10.5 (52.8-86.5)
Body mass index	25.5 ± 2.1 (22.1-29.5)
Complications, n	
Meniscal tear	10
Other	0
Follow-up period, mo	14.4 ± 3.4 (12-23)

RESULTS

Patient Characteristics

A total of 17 patients (17 knees) were enrolled in this study. There were 5 men and 12 women, with a mean age of 58.4 years at the time of surgery. The mean body mass index was 25.5.<sup>36</sup> Participant characteristics are shown in Table 1. The mean opening angle was 12.0° (range, 7°-19°), and the mean opening width was 12.1 mm (range, 7-19 mm). There were 10 knees with meniscal tears; however, there were no severe postoperative complications such as infection and nonunion.

Primary Outcomes: CT Osteoabsorptiometry

Preoperatively, the %HDA was significantly higher in the femoral MN than in the femoral LN and LT ( $P < .015$ ) and was significantly higher in the patellar MLF than in the patellar MF ( $P = .001$ ). When comparing values pre- and post-OWHTO, we found that the %HDA in the femoral LN and LT as well as in the patellar MLF significantly increased after OWHTO ( $P = .038$ ,  $P = .003$ , and  $P = .020$ , respectively). The %HDA in the femoral MT and the patellar LLF significantly decreased after OWHTO ( $P = .042$  and  $P = .013$ , respectively) (Table 2).

Secondary Outcomes: Radiological Evaluation

The test-retest reliability of the radiological measurements was excellent in all cases. Table 3 shows the ICCs and 95% CIs for each measurement.

Regarding the pre- to postoperative changes in the coronal alignment of the knee, the FTA significantly changed from 179° to 170°, and the WBL significantly changed from 23.1% to 71.2% ( $P < .0001$  for both). Regarding the PF joint, the Blackburne-Peel ratio significantly changed from 0.80 to 0.66, and the tilting angle of the patella significantly changed from 8.6° to 4.8° ( $P < .0001$  for both). Radiologic findings revealed that OA progression in the TF joint was not significant. Preoperatively, the medial TF OA was reported as grade 2 in 3 knees, grade 3 in 13 knees, and grade 4 in 1 knee, whereas after surgery, the OA grade had improved in 1 knee. Regarding the PF joint, significant OA

TABLE 2  
Mean %HDA of Each Region of the Femoral Trochlea and the Patella Pre- and Postoperatively<sup>a</sup>

%HDA	Pre-OWHTO	Post-OWHTO	P Value
Femoral trochlea			
MT	26.0 ± 32.7	9.1 ± 9.7	<b>.042</b>
MN	47.4 ± 28.5	40.2 ± 19.6	.362
LN	23.9 ± 19.6	37.7 ± 23.6	<b>.038</b>
LT	2.7 ± 5.1	13.1 ± 13.6	<b>.003</b>
Patella			
MF	9.7 ± 12.2	8.1 ± 9.1	.576
CR	22.8 ± 20.7	22.8 ± 19.0	.995
MLF	41.0 ± 24.2	53.9 ± 20.2	<b>.020</b>
LLF	26.3 ± 24.7	15.2 ± 16.3	<b>.013</b>

<sup>a</sup>Data are reported as mean ± SD. Bolded P values indicate statistically significant difference between groups ( $P < .05$ ). CR, central ridge; %HDA, percentage of high-density area; LLF, lateral portion of lateral facet; LN, lateral notch; LT, lateral trochlea; MF, medial facet; MLF, medial portion of lateral facet; MN, medial notch; MT, medial trochlea; OWHTA, open-wedge high tibial osteotomy.

TABLE 3  
Test-Retest Reliability of the Radiologic Measurements<sup>a</sup>

Variable	ICC (95% CI)
Femorotibial angle	0.958 (0.899-0.976)
Weightbearing line	0.970 (0.926-0.982)
Posterior tibial slope	0.903 (0.770-0.943)
Insall-Salvati ratio	0.986 (0.966-0.992)
Blackburne-Peel ratio	0.928 (0.828-0.958)
Tilting angle	0.984 (0.962-0.991)
Lateral shift	0.994 (0.984-0.996)
Congruence angle	0.997 (0.993-0.998)

<sup>a</sup>ICC, intraclass correlation coefficient.

progression was found in 4 knees (24%) at the final follow-up ( $P = .041$ ) (Table 4).

DISCUSSION

The important findings of the present study were that the OWHTO procedure significantly increased stress distribution patterns of the LN and LT of the femur and the MFL of the patella. In addition, OWHTO significantly decreased the patellar height and significantly decreased the patellar tilting angle after surgery.

It is generally accepted that OWHTO with an ascending tibial tubercle osteotomy decreases the patellar height, which potentially leads to AKP, crepitus, extension lag, and decreased range of motion.<sup>14,35</sup> Our study presented a statistically significant decrease of the patellar height and degradation of the PF cartilage after OWHTO. OWHTO is often associated with decreased patellar height due to distal and lateral movement of the tibial tuberosity. Furthermore, lower patellar height potentially increases the load of

TABLE 4  
Radiologic Examination Results Between Pre- and Post-OWHTO<sup>a</sup>

Variable	Pre-OWHTO	Post-OWHTO	P Value
Femorotibial angle, deg	178.8 ± 2.6	169.8 ± 1.8	<.0001
Weightbearing line, %	23.1 ± 13.4	71.2 ± 6.3	<.0001
Posterior tibial slope, deg	9.0 ± 2.1	9.5 ± 2.5	.438
Insall-Salvati ratio	1.05 ± 0.14	1.06 ± 0.16	.542
Blackburne-Peel ratio	0.80 ± 0.10	0.66 ± 0.10	<.0001
Tilting angle, deg	8.6 ± 4.0	4.8 ± 4.0	<.0001
Lateral shift, %	12.5 ± 6.4	11.1 ± 6.5	.071
Congruence angle, deg	-9.4 ± 11.2	-6.9 ± 11.3	.239
Tibiofemoral OA, No. of knees <sup>b</sup>			.332
Grade 0	0	0	
Grade 1	0	0	
Grade 2	3	3	
Grade 3	13	14	
Grade 4	1	0	
Patellofemoral OA, No. of knees <sup>b</sup>			.041
Grade 0	5	2	
Grade 1	12	14	
Grade 2	0	1	
Grade 3	0	0	
Grade 4	0	0	

<sup>a</sup>Data are reported as mean ± SD unless otherwise indicated. Bolded P values indicate statistically significant difference between groups ( $P < .05$ ). OA, osteoarthritis; OWHTO, open-wedge high tibial osteotomy.

<sup>b</sup>According to the Kellgren-Lawrence<sup>15</sup> grading system.

the PF joint, resulting in PF OA and AKP.<sup>35</sup> Tigani et al<sup>38</sup> reported that  $>15^\circ$  of knee axis correction significantly decreased patellar height. Stoffel et al<sup>35</sup> reported that OWHTO led to a significant elevation in PF cartilage pressure at 30°, 60°, and 90° of knee flexion in a cadaveric biomechanical experiment. Some other radiologic and biomechanical studies have indicated an increase of PF contact pressure and the progression of PF OA after OWHTO. However, the distribution pattern of PF contact pressure after OWHTO remains unclear. Our results confirmed the observations of decreased patellar height as a result of OWHTO possibly causing the elevation or imbalance the contact stress of the surface of the PF joint.

There is a lack of consensus regarding changes in patellar tilt after OWHTO.<sup>8,16,40</sup> Our radiographic results were almost identical to those in a previous cadaveric study,<sup>8</sup> strongly suggesting that the medial tilt of the patella occurred because of a lateral shift of the tibial tuberosity forcing up the lateral side of the femur and patella in vivo (Figure 4). To evaluate the effect of OWHTO for an actual loading condition of the PF joint, a reasonable analytical approach is to predict the characteristics of stress distribution based on in vivo imaging data obtained from living participants. These results predicted that the distribution pattern of the subchondral bone density across the PF joint surface after OWHTO should be shifted laterally compared with that before

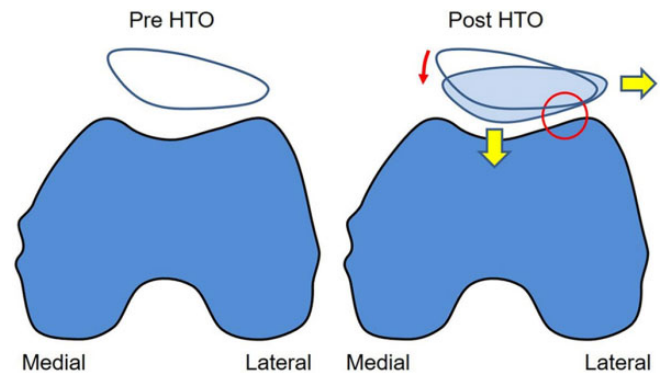


**Figure 4.** The mechanism whereby the compressive force on the lateral side of the patella is increased after open-wedge high tibial osteotomy (OWHTO). Lateral and distal shift of the tibial tubercle increased the pressure between the lateral patellar facet and the lateral wall of the trochlea (yellow arrows) and forced up the lateral groove (red circle), leading to a medial tilt of the patella (red arrow).

surgery. The results obtained using CT osteoabsorptiometry proved this hypothesis in vivo.

There were some limitations to the present study. First, the results were based on indirect measurement of stress acting on the PF joint. Therefore, the absolute value of the stress was not fully elucidated. Second, stress distributions across a joint are mainly determined by loading conditions and joint geometry. Although this study showed relationships between stress distributions and long-term loading conditions through the PF joint, the effects of the PF geometry on stress distribution should be clarified. Third, the number of participants was small. Power analysis indicated that at least 5 participants would be required to detect this effect size with 90% power and a significance of  $\alpha = .05$ . We therefore used this study design with a sample size of 17 participants. Fourth, the mean follow-up period was too short. We should perform a long-term follow-up study in the future to clarify the stress distribution across the PF joint after OWHTO. Fifth, the current study analyzed imaging data from patients before and after OWHTO. To confirm the effects of altered knee alignment on stress distribution across the PF joint, more CT image data should be collected from different participants undergoing other osteotomies or having other levels of knee deformities including valgus alignment.

## CONCLUSION

This study clearly demonstrated that the OWHTO procedure significantly increased stress distribution patterns of the femoral lateral trochlea and the medial portion of the patellar lateral facet by decreasing the patellar height and decreasing the patellar tilting angle.

## REFERENCES

1. Birmingham TB, Giffin JR, Chesworth BM, et al. Medial opening wedge high tibial osteotomy: a prospective cohort study of gait,

- radiographic, and patient-reported outcomes. *Arthritis Rheum.* 2009; 61(5):648-657.
2. Blackburne JS, Peel TE. A new method of measuring patellar height. *J Bone Joint Surg Br.* 1977;59(2):241-242.
  3. Brouwer RW, Bierma-Zeinstra SM, van Koeveeringe AJ, Verhaar JA. Patellar height and the inclination of the tibial plateau after high tibial osteotomy: the open versus the closed-wedge technique. *J Bone Joint Surg Br.* 2005;87(9):1227-1232.
  4. Cheriau JJ, Kapadia BH, Banerjee S, Jauregui JJ, Issa K, Mont MA. Mechanical, anatomical, and kinematic axis in TKA: concepts and practical applications. *Curr Rev Musculoskelet Med.* 2014;7(2):89-95.
  5. Eckstein F, Lohe F, Muller-Gerbl M, Steinlechner M, Putz R. Stress distribution in the trochlear notch: a model of bicentric load transmission through joints. *J Bone Joint Surg Br.* 1994;76(4):647-653.
  6. Eckstein F, Muller-Gerbl M, Steinlechner M, Kierse R, Putz R. Subchondral bone density in the human elbow assessed by computed tomography osteoabsorptiometry: a reflection of the loading history of the joint surfaces. *J Orthop Res.* 1995;13(2):268-278.
  7. Funakoshi T, Furushima K, Momma D, et al. Alteration of stress distribution patterns in symptomatic valgus instability of the elbow in baseball players: a computed tomography osteoabsorptiometry study. *Am J Sports Med.* 2016;44(4):989-994.
  8. Gaasbeek R, Welsing R, Barink M, Verdonshot N, van Kampen A. The influence of open and closed high tibial osteotomy on dynamic patellar tracking: a biomechanical study. *Knee Surg Sports Traumatol Arthrosc.* 2007;15(8):978-984.
  9. Goshima K, Sawaguchi T, Sakagoshi D, Shigemoto K, Hatsuchi Y, Akahane M. Age does not affect the clinical and radiological outcomes after open-wedge high tibial osteotomy. *Knee Surg Sports Traumatol Arthrosc.* 2017;25(3):918-923.
  10. Goshima K, Sawaguchi T, Shigemoto K, Iwai S, Nakanishi A, Ueoka K. Patellofemoral osteoarthritis progression and alignment changes after open-wedge high tibial osteotomy do not affect clinical outcomes at mid-term follow-up. *Arthroscopy.* 2017;33(10):1832-1839.
  11. Goutallier D, Delepine G, Debeyre J. The patello-femoral joint in osteoarthritis of the knee with genu varum. Article in French. *Rev Chir Orthop Reparatrice Appar Mot.* 1979;65(1):25-31.
  12. Insall J, Salvati E. Patella position in the normal knee joint. *Radiology.* 1971;101(1):101-104.
  13. Iwasaki N, Minami A, Miyazawa T, Kaneda K. Force distribution through the wrist joint in patients with different stages of Kienbock's disease: using computed tomography osteoabsorptiometry. *J Hand Surg Am.* 2000;25(5):870-876.
  14. Kaper BP, Bourne RB, Rorabeck CH, Macdonald SJ. Patellar infera after high tibial osteotomy. *J Arthroplasty.* 2001;16(2):168-173.
  15. Kellgren JH, Lawrence JS. Radiological assessment of osteoarthrosis. *Ann Rheum Dis.* 1957;16(4):494-502.
  16. Lee YS, Lee SB, Oh WS, Kwon YE, Lee BK. Changes in patellofemoral alignment do not cause clinical impact after open-wedge high tibial osteotomy. *Knee Surg Sports Traumatol Arthrosc.* 2016;24(1):129-133.
  17. Lobenhoffer P, Agneskirchner JD. Improvements in surgical technique of valgus high tibial osteotomy. *Knee Surg Sports Traumatol Arthrosc.* 2003;11(3):132-138.
  18. Lucas NP, Macaskill P, Irwig L, Bogduk N. The development of a quality appraisal tool for studies of diagnostic reliability (QAREL). *J Clin Epidemiol.* 2010;63(8):854-861.
  19. Merchant AC, Mercer RL, Jacobsen RH, Cool CR. Roentgenographic analysis of patellofemoral congruence. *J Bone Joint Surg Am.* 1974; 56(7):1391-1396.
  20. Momma D, Iwasaki N, Oizumi N, et al. Long-term stress distribution patterns across the elbow joint in baseball players assessed by computed tomography osteoabsorptiometry. *Am J Sports Med.* 2011; 39(2):336-341.
  21. Moore TM, Harvey JP Jr. Roentgenographic measurement of tibial-plateau depression due to fracture. *J Bone Joint Surg Am.* 1974;56(1): 155-160.
  22. Moreland JR, Bassett LW, Hanker GJ. Radiographic analysis of the axial alignment of the lower extremity. *J Bone Joint Surg Am.* 1987; 69(5):745-749.
  23. Müller-Gerbl M, Putz R, Hodapp N, Schulte E, Wimmer B. Computed tomography-osteabsorptiometry for assessing the density distribution of subchondral bone as a measure of long-term mechanical adaptation in individual joints. *Skeletal Radiol.* 1989; 18(7):507-512.
  24. Müller-Gerbl M, Putz R, Hodapp NH, Schulta E, Wimmer B. Computed tomography-osteabsorptiometry: a method of assessing the mechanical condition of the major joints in a living subject. *Clin Biomech (Bristol, Avon).* 1990;5(4):193-198.
  25. Niemeyer P, Koestler W, Kaehny C, et al. Two-year results of open-wedge high tibial osteotomy with fixation by medial plate fixator for medial compartment arthritis with varus malalignment of the knee. *Arthroscopy.* 2008;24(7):796-804.
  26. Nishida K, Iwasaki N, Fujisaki K, et al. Distribution of bone mineral density at osteochondral donor sites in the patellofemoral joint among baseball players and controls. *Am J Sports Med.* 2012;40(4):909-914.
  27. Oizumi N, Suenaga N, Minami A, Iwasaki N, Miyazawa T. Stress distribution patterns at the coracoacromial arch in rotator cuff tear measured by computed tomography osteoabsorptiometry. *J Orthop Res.* 2003;21(3):393-398.
  28. Onodera J, Kondo E, Omizu N, Ueda D, Yagi T, Yasuda K. Beta-tricalcium phosphate shows superior absorption rate and osteoconductivity compared to hydroxyapatite in open-wedge high tibial osteotomy. *Knee Surg Sports Traumatol Arthrosc.* 2014;22(11): 2763-2770.
  29. Onodera T, Majima T, Iwasaki N, Kamishima T, Kasahara Y, Minami A. Long-term stress distribution patterns of the ankle joint in varus knee alignment assessed by computed tomography osteoabsorptiometry. *Int Orthop.* 2012;36(9):1871-1876.
  30. Osti M, Gohm A, Schlick B, Benedetto KP. Complication rate following high tibial open-wedge osteotomy with spacer plates for incipient osteoarthritis of the knee with varus malalignment. *Knee Surg Sports Traumatol Arthrosc.* 2015;23(7):1943-1948.
  31. Saito T, Kumagai K, Akamatsu Y, Kobayashi H, Kusayama Y. Five- to ten-year outcome following medial opening-wedge high tibial osteotomy with rigid plate fixation in combination with an artificial bone substitute. *Bone Joint J.* 2014;96-B(3):339-344.
  32. Sasaki T, Yagi T. Subluxation of the patella: investigation by computerized tomography. *Int Orthop.* 1986;10(2):115-120.
  33. Sato D, Kondo E, Yabuuchi K, et al. Assessment of valgus laxity after release of the medial structure in medial open-wedge high tibial osteotomy: an in vivo biomechanical study using quantitative valgus stress radiography. *BMC Musculoskelet Disord.* 2019;20(1):481.
  34. Stäubli AE, De Simoni C, Babst R, Lobenhoffer P. TomoFix: a new LCP-concept for open wedge osteotomy of the medial proximal tibia—early results in 92 cases. *Injury.* 2003;34(suppl 2):B55-B62.
  35. Stoffel K, Willers C, Korshid O, Kuster M. Patellofemoral contact pressure following high tibial osteotomy: a cadaveric study. *Knee Surg Sports Traumatol Arthrosc.* 2007;15(9):1094-1100.
  36. Tanaka H, Kokubo Y. Epidemiology of obesity in Japan. *Japan Med Assoc J.* 2005;48(1):34-41.
  37. Tang WM, Zhu YH, Chiu KY. Axial alignment of the lower extremity in Chinese adults. *J Bone Joint Surg Am.* 2000;82(11):1603-1608.
  38. Tigani D, Ferrari D, Trentani P, Barbanti-Brodano G, Trentani F. Patellar height after high tibial osteotomy. *Int Orthop.* 2001;24(6): 331-334.
  39. Yabuuchi K, Kondo E, Onodera J, et al. Clinical outcomes and complications during and after medial open-wedge high tibial osteotomy using a locking plate: a 3 to 7-year follow-up study. *Orthop J Sports Med.* 2020;8(6):2325967120922535.
  40. Yang JH, Lee SH, Nathawat KS, Jeon SH, Oh KJ. The effect of biplane medial opening wedge high tibial osteotomy on patellofemoral joint indices. *Knee.* 2013;20(2):128-132.